npj | parkinson's disease

Article

Published in partnership with the Parkinson's Foundation

https://doi.org/10.1038/s41531-025-01074-0

Diffusion–tensor MRI study of the relationship between glymphatic system asymmetry and onset lateralization in Parkinson's disease

Zihan Li[1,6], Xinxin Miao[1,6], Qiumei Zhang[2,6], Jun Shen[3,6], Yongfeng Jia[1], Shaoyun Ge[4], Peixian Ji[1], Jianwei Wang[1], Kezhong Zhang[5] & Min Wang[1] ✉

The characteristic asymmetric motor symptoms of Parkinson's disease (PD) may be associated with asymmetric deposition of α-synuclein. The impaired glymphatic system may promote pathological deposition of α-synuclein, leading to disease progression. The aim of this study was to investigate the function of the glymphatic system in PD patients with unilateral motor symptom onset using diffusion tensor image analysis along the perivascular spaces (DTI-ALPS) method, and to elucidate the relationship between glymphatic system asymmetry and the side of motor symptom onset. We conducted diffusion tensor imaging scans on 36 left-onset PD (LPD) patients, 27 right-onset PD (RPD) patients, and 49 healthy controls (HCs). Bilateral hemispheric ALPS indices were calculated to assess glymphatic function, and an asymmetry index (AI) was derived to quantify interhemispheric asymmetry in glymphatic function. Compared to HCs, RPD patients exhibited a significant reduction in the left ALPS index, while both left and right ALPS indices were significantly reduced in LPD patients. In both LPD patients and HCs, the right ALPS index was lower than the left, suggesting a natural leftward asymmetry. However, this asymmetry was diminished in RPD patients, as indicated by a lower AI. Moreover, in RPD patients, the Unified Parkinson's Disease Rating Scale Part III score showed a negative correlation with the left ALPS index and with AI. This study demonstrated that PD patients with lateralized motor symptom onset exhibit different patterns of glymphatic system function. The glymphatic system asymmetry may provide new insights into the mechanism underlying the lateralized onset of PD.

Parkinson's disease (PD) is a neurodegenerative disorder with bradykinesia, resting tremor, rigidity, and postural instability as the core motor symptoms[1,2]. A defining feature of PD is the asymmetric onset of symptoms. PD patients tend to initially present with unilateral limb motor abnormalities[3,4], although the disease clinically progresses to bilateral involvement, the symptomatic dominant side also exhibits more severe motor symptoms[5]. This asymmetry distinguishes PD from Parkinsonism syndromes and complicates clinical management. Notably, left-onset PD (LPD) and right-onset PD (RPD) patients often differ in disease progression[6], risk of cognitive decline[7], and response to treatment[8]. This asymmetry is of increasing interest to researchers and clinicians, and revealing the neural mechanisms behind it is critical to predicting disease progression and optimizing individualized treatment strategies.

Typical pathologic hallmarks of PD include progressive loss of substantia nigra dopaminergic neurons[9] and deposition of Lewy bodies[10], which are mainly composed of α-synuclein[11]. Clinicopathologic studies have shown that asymmetry in dopaminergic denervation is present and correlates with asymmetry in motor function[12]. This asymmetry in dopaminergic integrity

[1]Department of Radiology, The First Affiliated Hospital of Nanjing Medical University, Nanjing, China. [2]Department of Radiology, Nanjing Central Hospital, Nanjing, China. [3]Department of Neurology, Taizhou Fourth People's Hospital, Taizhou, China. [4]Department of Radiology, The First Affiliated Hospital of NingBo University, Ningbo, China. [5]Department of Neurology, The First Affiliated Hospital of Nanjing Medical University, Nanjing, China. [6]These authors contributed equally: Zihan Li, Xinxin Miao, Qiumei Zhang, Jun Shen. ✉e-mail: jsphwangmin@njmu.edu.cn

may be determined by the asymmetric deposition of α-synuclein[13,14]. In addition, the lateralized onset is influenced by the shorter disease duration, younger age at symptom onset, and a family history of other movement disorders[15].

Multimodal neuroimaging studies provide valuable insights into the asymmetry of PD symptoms. Study of the brain's structural morphology has revealed that PD patients exhibit more pronounced cortical atrophy in the left frontal region during the early stages of the disease. However, as the disease progresses, the rate of atrophy is higher in the right hemisphere region[16]. The side of onset has been demonstrated to affect the type of brain atrophy, with LPD patients exhibiting gray matter atrophy in the right primary sensory and motor cortex and paracentral lobule and bilateral parahippocampal gyrus, whereas RPD patients show gray matter atrophy predominantly in the left lingual gyrus[17]. Previous investigations using tract-based spatial statistics have demonstrated that white matter damage is more severe in RPD patients than in LPD patients[18,19], and that white matter asymmetry may predict the side of PD onset, which has been externally validated with good predictive results. Fixel-based analysis[20] has also revealed distinct patterns of white matter integrity in the LPD and RPD cohorts. Functional neuroimaging studies have shown that the topological properties of movement-related networks in LPD patients display significant alterations[21]. However, existing studies have primarily focused on structural or functional abnormalities in specific brain regions or networks. The systemic pathological mechanisms driving PD symptom asymmetry remain to be elucidated.

In 2012, the discovery of the cerebral glymphatic system by Iliff et al.[22] provided a new perspective on the study of neurodegenerative diseases. This system is responsible for removing metabolic waste products and neurotoxic substances via the exchange between cerebrospinal and interstitial fluid[23]. Subsequently, Taoka's team[24] introduced the "diffusion tensor image analysis along perivascular spaces" (DTI-ALPS) method, a non-invasive and quantitative approach to assess the function of the glymphatic system, which has been widely applied to study various neurodegenerative disorders[25–27]. Glymphatic clearance dysfunction may result in dopaminergic neuronal damage secondary to increased α-synuclein deposition. Several experimental studies on animals have demonstrated that a decreased glymphatic function may promote the accumulation of α-synuclein and exacerbate Parkinson's symptoms[28,29]. Therefore, evaluating the function of the glymphatic system may help elucidate the pathophysiologic mechanisms underlying PD. Previous studies have reported significantly lower DTI-ALPS index in PD patients compared to healthy controls, particularly among older individuals[30], those with more severe symptoms[31], and/or patients with sleep disturbances[32]. Moreover, Ma et al.[33] showed that the DTI-ALPS index was lower in advanced PD patients compared to HCs, with no significant differences observed between early PD patients and controls, suggesting a close association between PD progression and glymphatic dysfunction. However, most prior research has largely overlooked the potential hemispheric asymmetry in glymphatic dysfunction and has not thoroughly examined how these functional disparities relate to the lateralized onset of PD symptoms. Shen's study[34] demonstrated that glymphatic system impairment in PD patients may originate from the left hemisphere, providing preliminary evidence for the lateralization of the glymphatic system. They compared the left and right DTI-ALPS indices in both LPD and RPD patients, but no statistical difference was found. More detailed subgroup analysis comparing LPD and RPD patients with healthy controls may reveal further insights.

Therefore, the present study aimed to investigate glymphatic system function in PD patients with different onset sides, with a specific focus on potential hemispheric asymmetries. To further explore the relationship between the impairment of the glymphatic system and motor and non-motor symptoms, we also analyzed correlations between the DTI-ALPS index and clinical characteristics.

Results

Participant characteristics

This study included 36 LPD patients, 27 RPD patients, and 49 healthy controls. Statistical analysis revealed no significant differences among the three groups in terms of age, sex, or education duration ($p > 0.05$). Furthermore, the LPD and RPD groups showed no significant differences in disease duration, H&Y stage, or LEDD usage ($p > 0.05$). Detailed clinical characteristics, including motor symptoms, motor performance, mental and cognitive impairments, and sleep disorders between the two PD onset types are summarized in Table 1.

Inter- and intra-reader reliability

The DTI-ALPS indices and results of reliability analysis obtained after ROIs placement of the DTI images are presented in Table 2. The consistency of the ALPS indices obtained after ROIs were placed by two independent observers or by the same observer at different times was remarkable, with ICCs > 0.75.

DTI-ALPS index in PD patients and HCs

When comparing global ALPS indices (GALPS) between PD patients and controls, a significant difference was found between the three groups ($p = 0.003$). Post hoc comparisons revealed that compared to HCs, both LPD and RPD patients exhibited significantly lower global ALPS indices ($p = 0.011$, and $p = 0.001$, respectively). No significant difference was observed in the global ALPS index between LPD and RPD patients (Fig. 1c).

When comparing unilateral ALPS indices between PD patients and controls, a significant difference in the left ALPS index (LALPS) was observed between the three groups ($p = 0.002$), while no significant difference was found in the right ALPS index (RALPS) ($p = 0.051$). Post hoc comparisons revealed that in RPD patients, the left ALPS index was significantly decreased compared to HCs ($p < 0.001$), while the right ALPS index in RPD patients did not show a significant difference compared to HCs ($p = 0.059$) (Fig. 1a). In LPD patients, both the left ALPS index ($p = 0.026$) and the right ALPS index ($p = 0.031$) were significantly lower than those of HCs (Fig. 1b). No significant differences were observed in the left and right DTI-ALPS indices between LPD and RPD patients.

Asymmetry index in PD patients and HCs

Two-sample paired *t*-tests showed that the right ALPS index was lower than the left ALPS index in both LPD patients and HCs ($p = 0.001$, and $p < 0.001$, respectively) (Fig. 2b, c), indicating that the glymphatic system in both LPD patients and HCs was characterized by leftward asymmetry. However, RPD patients showed no significant difference in the ALPS index between the left and right hemispheres (Fig. 2a). In addition, the analysis of the asymmetry index (AI) indicators found that the AI was significantly lower in RPD patients compared to HCs ($p = 0.037$) (Fig. 1d), indicating that the leftward asymmetry in RPD patients was attenuated.

Correlations between clinical features and DTI-ALPS index and asymmetry index

After adjusting for age, sex, MMSE, and FAB scores, UPDRS-III scores were negatively correlated with the left ALPS index in all PD patients ($r = -0.265$, $p = 0.036$) (Fig. 3a), and UPDRS-III scores were also negatively correlated with both the left ALPS index ($r = -0.442$, $p = 0.035$) and AI ($r = -0.482$, $p = 0.020$) in RPD patients (Fig. 3b, c). Conversely, no significant correlations were observed between non-motor symptom scores and the left or right ALPS indices, nor with the AI in RPD patients. In LPD patients, no significant correlations were found between the DTI-ALPS index or AI and clinical scales.

Discussion

In this study, we conducted a comprehensive analysis of the bilateral hemispheric glymphatic system function in LPD and RPD patients to elucidate the relationship between glymphatic system dysfunction and clinically lateralized symptom onset. The main findings are summarized as follows: (1) We detected lower global DTI-ALPS indices in both PD subgroups compared to HCs, with RPD patients predominantly exhibiting left hemispheric glymphatic system dysfunction. (2) In the normal adult brain, the glymphatic system tends to exhibit leftward asymmetry, with the left hemisphere playing a dominant role. This pattern was also observed in LPD

Table 1 | Demographic and clinical characteristics of PD patients and controls

	PD		HCs	*P* value	
	LPD	RPD		LPD vs RPD	PD vs HCs
n	36	27	49		
Clinical variables					
Age (y)	62.64 ± 6.40	61.41 ± 7.35	63.39 ± 4.97	0.481	0.227
Gender (Male/Female)	21/15	15/12	30/19	0.825	0.663
Education duration (y)	10.42 ± 3.83	10.19 ± 4.10	11.40 ± 2.98	0.819	0.109
Disease duration (y)	5.65 ± 3.33	6.05 ± 3.75	NA	0.662	NA
H &Y stage	2.11 ± 0.75	2.11 ± 0.67	NA	0.986	NA
LEDD (mg/d)	725.00 (431.25, 981.25)	587.50 (328.13, 692.63)	NA	0.074	NA
Motor symptom					
UPDRS-III score	30.58 ± 16.31	30.89 ± 10.79	NA	0.933	NA
Bradykinesia score	15.13 ± 7.96	16.44 ± 6.44	NA	0.573	NA
Rigidity score	7.83 ± 3.81	8.28 ± 4.21	NA	0.721	NA
PIGD score	5.31 ± 4.38	5.33 ± 4.02	NA	0.980	NA
TD score	5.50 (2.00, 10.00)	4.50 (2.00, 9.00)	NA	0.823	NA
Motor performance					
TUG (s)	14.14 ± 4.63	11.70 ± 5.36	NA	0.066	NA
Tinetti Gait score	9.20 ± 2.82	8.93 ± 3.29	NA	0.725	NA
Tinetti Balance score	13.51 ± 3.74	13.78 ± 2.69	NA	0.758	NA
FOG score	1.00 (0.00, 10.00)	1.00 (0.00, 8.00)	NA	0.958	NA
Mental and cognitive impairment					
MMSE score	27.09 ± 2.30	28.07 ± 1.69	28.92 ± 1.06	0.067	<0.001*
FAB score	16.09 ± 1.84	15.85 ± 2.32	17.00 ± 1.07	0.659	0.003*
HARS score	11.71 ± 7.03	11.63 ± 7.66	3.35 ± 3.58	0.964	<0.001*
HDRS score	13.35 ± 10.81	13.32 ± 9.01	1.73 ± 2.27	0.992	<0.001*
AS score	14.14 ± 7.01	11.72 ± 4.91	NA	0.225	NA
Sleep disorders					
ESS score	8.00 (3.00, 12.00)	4.00 (3.00, 8.00)	NA	0.131	NA
PDSS score	122.81 ± 23.84	122.96 ± 23.46	NA	0.981	NA
RBDSQ score	4.92 ± 3.65	4.00 ± 3.17	NA	0.302	NA

Continuous variables are presented as mean ± standard deviation for parametric data and median (interquartile range) for nonparametric data.
PD Parkinson's disease, *LPD* Left-onset Parkinson's disease, *RPD* right-onset Parkinson's disease, *HCs* healthy controls, *y* years, *H&Y* Hoehn and Yahr, *LEDD* levodopa equivalent daily dose, *UPDRS* unified Parkinson's disease rating scale, *PIGD* postural instability/gait difficulty, *TD* tremor dominant, *TUG* timed up and go, *FOG* freezing of gait, *MMSE* mini-mental state examination, *FAB* frontal assessment battery, *HARS* Hamilton anxiety rating scale, *HDRS* Hamilton depression rating scale, *AS* apathy scale, *ESS* excessive daytime sleepiness scale, *PDSS* Parkinson's disease sleep scale, *RBDSQ* rapid sleep behavior disorder questionnaire, *NA* not applicable.

patients, while RPD patients showed attenuated leftward asymmetry. (3) Impaired motor performance in RPD patients was correlated with lower left ALPS index and reduced leftward asymmetry. The findings offer novel neurobiological insights into the laterality of PD onset, may provide new targets for personalized diagnosis and treatment.

Classical tracer studies[35] have demonstrated a significant association between the DTI-ALPS index and the clearance function of the glymphatic system. In our cohort, both LPD and RPD patients exhibited lower global DTI-ALPS indices compared to HCs, suggesting overall impaired glymphatic system function in PD patients, regardless of pathogenic laterality. As reported by Zou et al.[29], reduced glymphatic clearance has been implicated in the early pathological process of an A53T transgenic PD mouse model. The formation of reactive astrocytes caused by α-synuclein overexpression leads to impaired polarization of the water channel aquaporin-4 (AQP4), which may significantly contribute to glymphatic dysfunction in PD. Furthermore, studies have demonstrated that PD patients display an increased perivascular space (PVS) burden in the centrum semiovale and basal ganglia[36]. A greater PVS burden in the basal ganglia correlates with higher postural instability scores[37,38] and an elevated risk of progression to freezing of gait[39]. These findings suggest that glymphatic system dysfunction is a

Table 2 | Inter- and intra-reader ICCs for the measurements of parameters

Parameters	Inter-reader ICC	Intra-reader ICC
Left diffusivity (×10^{-3} mm^2/s)		
Dxxproj	0.957 (0.936–0.971)	0.912 (0.820–0.951)
Dxxasso	0.893 (0.823–0.933)	0.930 (0.899–0.952)
Dyyproj	0.903 (0.804–0.964)	0.876 (0.769–0.927)
Dzzasso	0.887 (0.831–0.923)	0.837 (0.717–0.901)
Left ALPS-index	0.899 (0.837–0.935)	0.934 (0.773–0.971)
Right diffusivity (×10^{-3} mm^2/s)		
Dxxproj	0.928 (0.897–0.950)	0.906 (0.861–0.937)
Dxxasso	0.881 (0.766–0.932)	0.849 (0.722–0.899)
Dyyproj	0.920 (0.789–0.960)	0.884 (0.776–0.934)
Dzzasso	0.886 (0.829–0.924)	0.844 (0.778–0.891)
Right ALPS-index	0.930 (0.753–0.969)	0.931 (0.746–0.970)

Data in parentheses are 95% confidence intervals.
ICC intra-class correlation coefficient

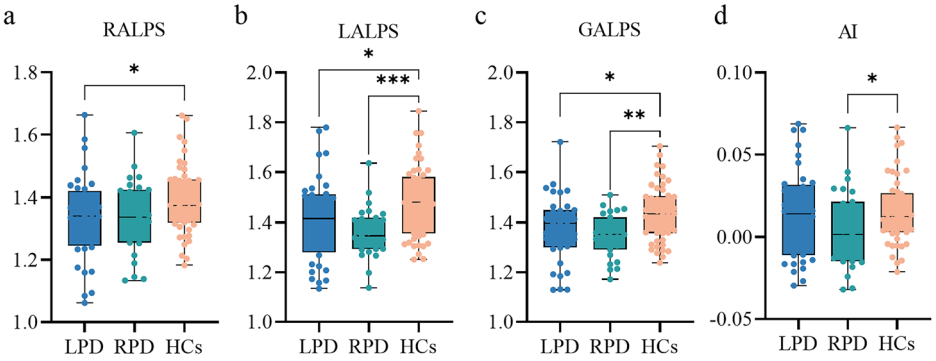

Fig. 1 | Box plots showing statistics of ALPS index and asymmetry index for LPD, RPD patients, and healthy controls. Differences between the three groups in **a** right ALPS, **b** left ALPS, **c** global ALPS, **d** asymmetry index. Error bars represent standard deviations. Statistical analyses were performed using one-way ANOVA followed by a post-hoc test for multiple comparisons. ALPS analysis along the perivascular space. $^{*}p < 0.05$, $^{**}p < 0.01$, $^{***}p < 0.001$.

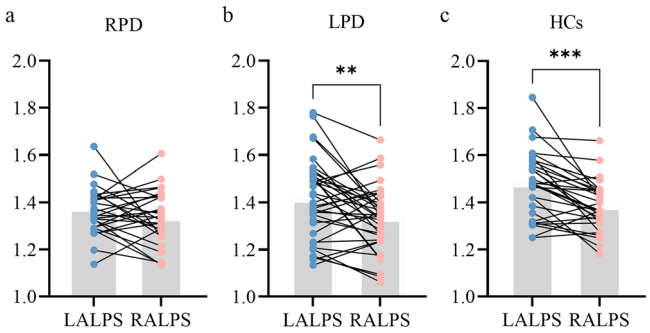

Fig. 2 | Comparison of left and right ALPS indices. The difference of ALPS indices between left and right sides in (**a**) RPD patients, **b** LPD patients, **c** Healthy controls. Error bars represent standard deviations. Statistical analyses were performed using two-sample paired t-test. $^{**}p < 0.01$, $^{***}p < 0.001$.

significant contributor to the pathogenesis and progression of PD. Nevertheless, the potential influence of the laterality of clinical symptom onset on glymphatic system impairment has been largely overlooked in previous research.

It is noteworthy that compared to HCs, both RPD and LPD patients showed significantly lower left ALPS index. Shen's[34] study noted that compared with HCs, early PD patients (H&Y ≤ 2) only exhibited lower ALPS index in the left hemisphere, whereas patients with intermediate to late stage (H&Y > 2) exhibited lower DTI-ALPS index in both cerebral hemispheres. This result is similar to our study and may indicate that glymphatic system impairment may originate from the left hemisphere. However, in our study, despite similar global ALPS indices between RPD and LPD patients, the right ALPS index was also lower in LPD patients compared to HCs. This suggests that the glymphatic system of LPD and RPD subtypes may follow distinct patterns of dysfunction despite comparable total pathological burdens. The differences in spatial distribution of impairment between these two subtypes imply the presence of distinct underlying pathophysiological mechanisms. Given the brain's contralateral control of motor function, glymphatic impairment in RPD patients is predominantly localized to the left hemisphere. In LPD patients, however, the right hemisphere also bears part of the burden of impairment, resulting in the impaired glymphatic system in both the left and right hemispheres. Interestingly, although the right limbs of LPD patients had not yet manifested clinical symptoms, glymphatic system dysfunction was already detectable, suggesting that impairments in the glymphatic system may precede the onset of motor symptoms in the contralateral limbs.

The population included in this study was right-handed. It is generally accepted that the left hemisphere is dominant in right-handed individuals[40], particularly in relation to motor control[41], language[42] and other cognitive functions. In RPD patients, the left hemisphere, as the dominant hemisphere, is not only responsible for a normally high level of metabolic activity but may also undergo compensatory activity due to disease-related dysfunction[34], thereby generating increased metabolic waste. However, due to potential impairment of the glymphatic system resulting from the disease, its efficiency in clearing metabolic waste may be compromised. This accumulation of waste products further increases the burden on the glymphatic system, thus resulting in a vicious cycle. The right hemisphere may maintain relative functional integrity in the early disease course due to less compensatory stress. In contrast, in LPD patients, the DTI-ALPS indices were decreased bilaterally, suggesting more extensive glymphatic system impairment. Prior studies in the right-handed PD population have demonstrated that LPD patients exhibit more extensive cortical thinning[17] and abnormal spontaneous brain activity than RPD patients[43], supporting the characteristic asymmetry pattern in PD. Our study further confirms the presence of lateralized dysfunction in PD patients, and the glymphatic system may be a potential contributor to this asymmetry.

After adjusting for potential confounders, our analysis revealed a negative correlation between UPDRS-III scores and left ALPS index in all PD patients. Previous study[44] has demonstrated that the DTI-ALPS index can be used to predict longitudinal motor function progression in PD patients. Similarly, a negative correlation between UPDRS-III score and left ALPS index was also observed in RPD patients, suggesting that more severe motor symptoms in RPD patients are associated with more pronounced dysfunction of the left hemispheric glymphatic system. This finding indicates that the left ALPS index may serve as a potential biomarker for motor symptom severity in RPD patients. However, no correlation between glymphatic system dysfunction and clinical scales was observed in LPD patients, which may be related to the disease stage in this cohort. Baumann et al.[45] found that motor symptoms progressed more slowly in LPD patients compared to RPD patients. The LPD patients included in this study were in the early to middle stages of the disease (H&Y: 2.11 ± 0.75), and impairment of glymphatic system exists in both cerebral hemispheres, rather than concentrated on one side, which may diffuse the direct effects of the pathological load on motor function and delay the emergence of a correlation between the clinical symptoms and glymphatic system dysfunction. It is possible that such a correlation may become apparent as the disease progresses. However, given that our study is cross-sectional, subsequent longitudinal follow-up is necessary to validate this hypothesis.

Interestingly, our study revealed that in healthy controls, the right ALPS index was lower than the left, indicating that the glymphatic system is dominant in the left hemisphere in normal adults[46], showing a natural leftward asymmetry. In contrast, in RPD patients, the asymmetry index was significantly lower compared to HCs, which may be attributed to glymphatic dysfunction in RPD patients that primarily affects the left hemisphere, preventing the brain from maintaining its normal leftward dominance. Although the DTI-ALPS indices were decreased bilaterally in LPD patients, the bilateral impairment may still exhibit a leftward asymmetry pattern similar to that observed in healthy individuals. Several studies have proposed that differences in cerebral vascular pulsation[47] and neuronal activity[48] in different hemispheres may affect glymphatic flow, and the finding of such asymmetrical attenuation only in RPD patients may also

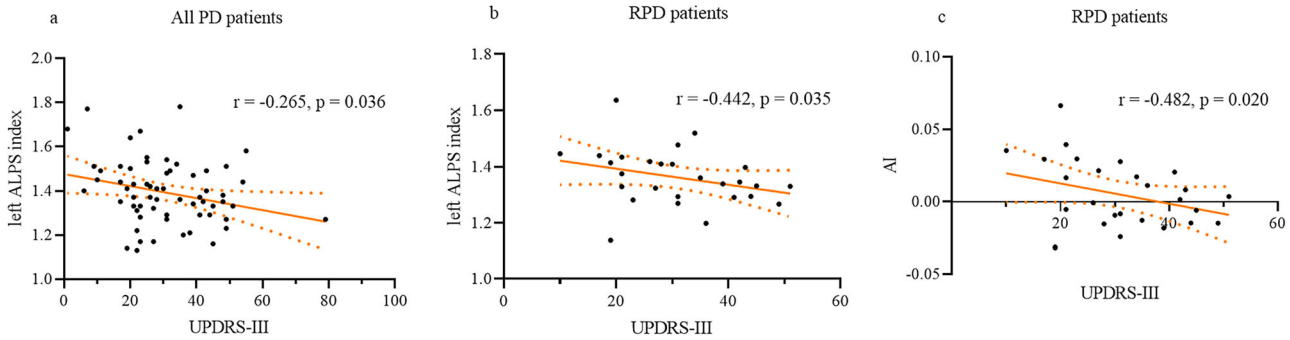

Fig. 3 | Correlation between the altered ALPS index, asymmetry index, and clinical scores in PD patients. Left ALPS index correlated significantly with UPDRS-III in: **a** all PD patients, and **b** RPD patients. **c** AI correlated significantly with UPDRS-III in RPD patients. AI asymmetry index, UPDRS unified Parkinson's disease rating scale.

suggest that the disease affects glymphatic function in a different way in two subtypes of PD patients. Moreover, the negative correlation between the asymmetry index and UPDRS-III score in RPD patients suggests a relationship between reduced leftward asymmetry and the severity of motor symptoms, and the asymmetry index may be helpful in the early identification of RPD patients.

No association between non-motor symptoms and the glymphatic system in PD patients with different motor onset sides was found in our study. This lack of correlation may be attributed to the use of rapid cognitive screening scales such as MMSE, which primarily evaluate overall cognitive status[49]. While cognitive functions encompass attention, executive function, memory, language, and spatial perception[50], previous literature suggests that lateralized cognitive changes in PD patients predominantly affect memory domains[7,51]. Thus, employing more sensitive neuropsychological tests to equally assess lateralization in both hemispheres may enhance the detection of latent, progressively lateralized patterns of cognitive decline in PD patients.

This study has several limitations. First, as a cross-sectional study, all included PD patients were in the early to mid-stage of the disease, and the sample size was relatively small. Future multicenter studies with larger sample sizes are needed to classify RPD and LPD patients into early and late-stage patients for detailed subgroup analyses, and to validate our findings by observing the dynamics of the left and right hemispheric DTI-ALPS indices of LPD and RPD patients through longitudinal follow-up. Second, since the patients in this study were collected between 2016 and 2019, lateralization scores from the UPDRS-III were not counted, and the laterality of motor symptom onset was confirmed by medical history, clinical presentation, and neurological examination. Distinguishing between UPDRS-III subscales such as left/right tremor, rigidity, and bradykinesia, and exploring their associations with the DTI-ALPS index may be more helpful in accurately exploring the relationship between DTI-ALPS indices and specific motor symptoms. Third, further research is needed to investigate the potential therapeutic implications of targeting the glymphatic system in PD. For example, strategies aimed at improving glymphatic clearance, such as enhancing sleep quality or modulating cerebrospinal fluid flow, could potentially slow disease progression or alleviate symptom severity. Finally, the function of the glymphatic pathway is significantly influenced during sleep, and given the high prevalence of sleep disturbances in PD patients, future studies should specifically examine glymphatic system dysfunction in those experiencing concurrent sleep disorders.

In conclusion, PD patients with different sides of symptom onset exhibit distinct patterns of glymphatic system dysfunction. RPD patients exhibit primarily impaired glymphatic system in the left hemisphere, whereas LPD patients show bilateral glymphatic system impairment. Both normal adults and LPD patients present a leftward asymmetry in glymphatic system function, a characteristic that is diminished in RPD patients. The asymmetry of glymphatic system impairment may be a contributing factor to the clinical laterality onset of PD.

Methods

Study population

Between May 2016 and August 2019, we recruited 63 PD patients. The following inclusion criteria were applied: (1) Idiopathic PD diagnosed according to the UK Parkinson's Disease Society Brain Bank criteria; (2) right-handed; (3) no family history. Exclusion criteria: (1) patients with parkinsonism-plus syndrome such as multiple system atrophy and progressive supranuclear palsy; (2) the presence of previous cerebral hemorrhage, cerebral infarction, craniocerebral trauma, history of tumor and history of craniocerebral surgery; (3) a history of drug abuse, alcoholism or syncope; (4) contraindications to MRI scanning; (5) severe artifacts on MRI images; (6) data sets without T1-weighted images or DTI images. The laterality of motor symptom onset was confirmed by a combination of medical history, clinical presentation, and supplemented by neurological examination; patients who had bilateral onset or whose side of onset could not be consistently confirmed were excluded, thus classifying PD patients as LPD ($n = 36$) or RPD ($n = 27$). Meanwhile, 49 healthy controls matched for age, sex, and hand use habits, and with no history of neurological or psychiatric disorders, were enrolled (Fig. 4).

All PD patients underwent MRI scanning and clinical scale assessments in the "off" state approximately 12 h after discontinuing all anti-Parkinsonian medications. The severity of the disease was assessed by the Hoehn and Yahr (H&Y) stage. Using the Unified Parkinson's Disease Rating Scale (UPDRS) to assess motor function. Postural Instability/Gait Difficulty (PIGD), Tremor Dominant (TD), bradykinesia score, rigidity score, Timed Up and Go (TUG), Tinetti Mobility Test (TMT), and Freezing of Gait Questionnaire (FOGQ) were used to assess motor performance. In addition, using the Mini-Mental State Examination (MMSE) and, Frontal Assessment Battery (FAB) to assess cognitive and executive function. Hamilton Depression Rating Scale (HDRS), Hamilton Anxiety Rating Scale (HARS), and Apathy Scale (AS) were used to screen for the presence of mental disorders. Excessive Daytime Sleepiness Scale (ESS), Parkinson's Disease Sleep Scale (PDSS), and Rapid Sleep Behavior Disorder Questionnaire (RBDSQ) were used to assess sleep quality and sleep disorders. Levodopa equivalent daily dose (LEDD) was calculated based on the equivalent dose conversion standard established by the Movement Disorder Society (MDS)[52]. The general formula applied was: LEDD = drug dose × proportion of drug taken × number of doses × conversion factor. The following antiparkinsonian medications are commonly used in our hospital: Madopar, drug dose 200 mg; conversion factor 1; Sinemet, drug dose 200 mg, conversion factor 0.75; Selegiline, drug dose 5 mg, conversion factor 10; Rasagiline, drug dose 1 mg, conversion factor 100; piribedil, drug dose 50 mg, conversion factor 1; Pramipexole, drug dose 0.25 mg, conversion factor 100; Amantadine, drug dose 100 mg, conversion factor 1; Entacapone, the equivalent dose of levodopa taken at the same time × 0.33.

The study was approved by the ethics committee of the First Affiliated Hospital of Nanjing Medical University (2014-SRFA-097). Written

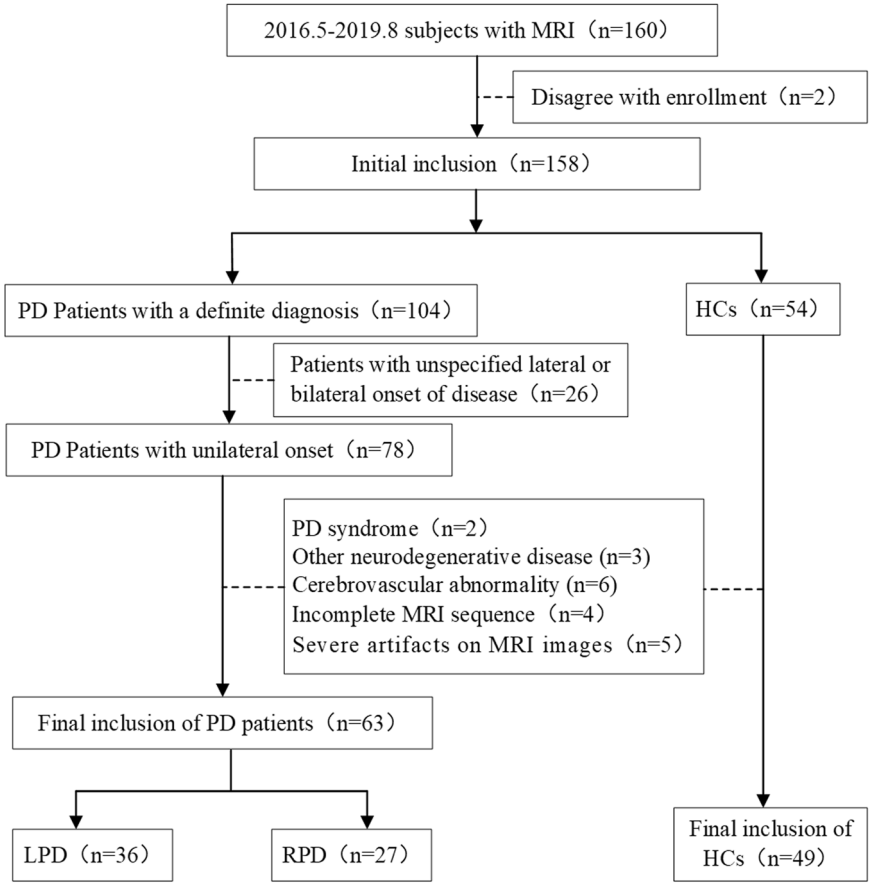

Fig. 4 | The flowchart of inclusion, exclusion criteria, and grouping of the study cohort. Among the 160 participants (between 2016 and 2019), 2 participants were excluded due to refusal of enrollment. The cohort included 104 patients with confirmed PD diagnosis and 54 healthy controls. 26 PD patients with unspecified lateral or bilateral onset were excluded, 20 participants were excluded due to (PD syndrome: $n = 2$; Other neurodegenerative disease: $n = 3$; Cerebrovascular abnormality: $n = 6$; Incomplete MRI sequence: $n = 4$; Severe artifacts on MRI images: $n = 5$). Finally, 63 PD patients and 49 healthy controls were included. PD patients were further divided into LPD ($n = 36$) and RPD ($n = 27$) subgroups.

informed consent was obtained from all participants to authorize the retrospective use of their previously collected clinical records and imaging data for medical research. All procedures complied with the ethical standards of the institutional review board and the 1964 Declaration of Helsinki and its later amendments.

Data acquisition

Participants were scanned using a Siemens 3.0 Tesla MAGNETOM Verio MRI scanner from Germany, equipped with an eight-channel phased array head coil. To minimize head motion, foam padding was utilized, and earplugs were used to mitigate the intrusion of ambient noise. For the DTI sequence, axial images were captured using a spin echo-planar imaging technique, set with the following parameters: repetition time (TR) = 9800 ms, echo time (TE) = 95 ms, field of view (FOV) = 256 × 256 mm^2, slice thickness = 2 mm with no slice gap, matrix size = 128 × 128. In the initial phase of acquisition, diffusion weighting was not applied ($b = 0$ s/mm^2); subsequently, a diffusion gradient was introduced across 30 noncollinear directions with a weighting factor of $b = 1000$ s/mm^2. A magnetization-prepared rapid gradient-echo sequence was employed for acquiring three-dimensional T1-weighted images, with the following parameters: TR = 1900 ms, TE = 2.95 ms, flip angle = 9°, FOV = 256 × 256 mm^2, slice thickness = 1 mm, matrix size = 256 × 256, and voxel size = 1 × 1 × 1 mm^3. Susceptibility-weighted imaging (SWI) scanning parameters: A high-resolution 3D fast low-angle shot sequence was used, with a TR of 28 ms, a TE of 20 ms, a flip angle of 15°, a FOV of 230 × 180 mm^2, and a FOV orientation of 78.1%. The intensity map, corrected phase map, minimum intensity projection, and SWI map were automatically obtained by SWI post-processing software. All the MR scans were conducted in parallel with the anterior–posterior commissural plane.

Preprocessing of DTI and DTI-ALPS index calculation

The FSL software (version 6.0.1, FMRIB Software Library; http://www.fmrib.ox.ac.uk/fsl/) was employed to preprocess the DTI dataset. Initially, raw DTI images were corrected to address eddy current distortions and motion artifacts, and the skull and non-brain tissue were removed. Diffusivity maps were subsequently generated in directions of *x*-, *y*-, and *z*-axis (Dx, Dy, Dz) for each subject. According to SWI, the medullary vein can be seen traveling along the horizontal *x*-axis and perpendicular to the lateral ventricle in the section of the lateral ventricle body (Fig. 5b). The projection fibers next to the lateral ventricle ran in the *z*-axis direction, the association fibers ran in the *y*-axis direction, the perivascular space is perpendicular to both the projection fibers and the association fibers (Fig. 5c). Consequently, the diffusivity of the projection fibers and the association fibers along the *x*-axis in this region can be considered a partial representation of the water diffusivity along the direction of the perivascular space. Using the FSL eyes tool, based on color-coded fractional anisotropy (FA) maps and SWI images, two experienced neuroradiologists placed 4-mm-diameter spherical regions of interest (ROIs) within the projection fibers and association fibers near the medullary veins of the bilateral cerebral hemispheres, and extracted diffusion coefficients of these ROIs along the different directions (Fig. 5a). ROIs were placed at three consecutive levels. One month after the initial assessment, reader1 reassessed all images in random order. To assess the reliability and reproducibility of quantitative MRI measurements, we used the intraclass correlation coefficient (ICC) and its 95% confidence intervals to quantify inter-observer and intra-observer agreement.

The DTI-ALPS index was calculated = mean (Dxxproj, Dxxassoc)/mean (Dyyproj, Dzzassoc). The left ALPS (LALPS) index and the right ALPS (RALPS) represent the left and right hemispheric ALPS indices, respectively. The global ALPS (GALPS) index was defined as follows: GALPS index = (LALPS + RALPS)/2. The asymmetry index (AI) was

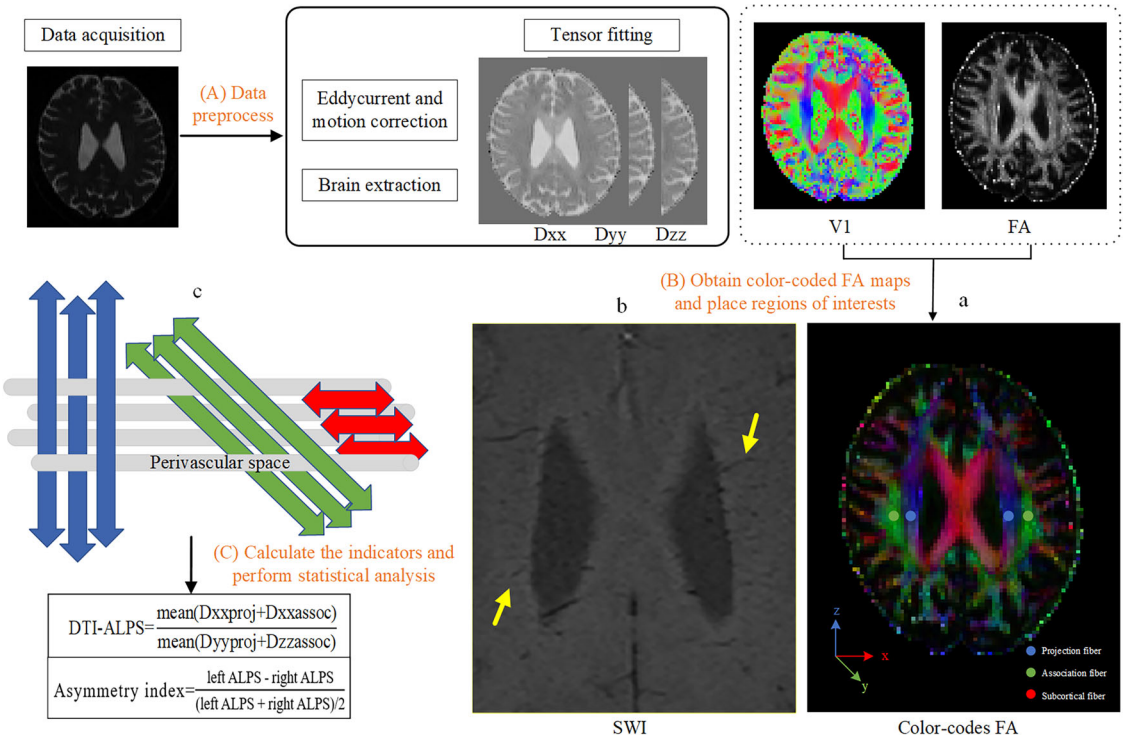

Fig. 5 | Illustration of the diffusion tensor image analysis along the perivascular space (DTI-ALPS) method. a DTI data preprocessing; **b** acquisition of color-coded FA maps and placement of regions of interest to measure the diffusivity of projection and association fibers. The blue, green, and red areas in the DTI color map represent the location of projection fibers (z-axis), association fibers (*y*-axis), and subcortical fibers (x-axis), respectively. The placement was confirmed by SWI, which showed that the medullary veins run perpendicular to the ventricular wall (yellow arrow). The gray cylinder shows the perivascular gap of the medullary vein, and the arrows show the main directions of the projection fibers (blue), association fibers (green), and subcortical fibers (red); **c** calculation of ALPS index and asymmetry index for statistical analysis. FA fractional anisotropy; SWI susceptibility-weighted imaging; ALPS analysis along the perivascular space.

calculated = (LALPS-RALPS)/GALPS to further quantify the degree of asymmetry between the left and right hemispheric ALPS indices (Fig. 5).

Statistical analysis

The Shapiro–Wilk normality test was used to test the normality of variable distribution. Variables that were approximately normally distributed were presented as mean ± standard deviation, and two-sample *t*-tests were used for comparisons between groups; variables that did not conform to the normal distribution were expressed as median (interquartile range), and Mann–Whitney *U*-tests were used for comparisons between groups. The chi-square test was used to examine sex distribution. Inter- and intra-observer agreement on the DTI-ALPS index was assessed by the inter- and intra-class correlation coefficients, with ranges and interpretations as follows: 0.75–1.00 (remarkable consistency), 0.40–0.74 (medium consistency), 0.00–0.39 (poor consistency). One-way analysis of variance (ANOVA) was applied to compare the DTI-ALPS index and AI among the LPD, RPD, and HCs groups, followed by post hoc analysis to further compare differences between groups and correct for multiple comparisons. Differences in the left and right ALPS indices between the three groups were compared using a two-sample paired *t*-test. Partial correlation analysis was used to examine the association between the left and right ALPS indices, asymmetry index, and motor performance after adjusting for age, sex, MMSE, and FAB scores. Statistical significance was defined at a threshold of $p < 0.05$. All statistical analyses were performed using SPSS software (version 26, IBM-SPSS; https://www.ibm.com/cn-zh/spss).

Data availability

Clinical and neuroimaging data can be shared on reasonable request from qualified investigators by contacting the corresponding authors to the extent permitted by the Research Ethics Committee.

Code availability

The DTI data were processed using FSL (version 6.0.1, FMRIB Software Library; http://www.fmrib.ox.ac.uk/fsl/). Statistical analyses were performed using SPSS (version 26, IBM-SPSS; https://www.ibm.com/cn-zh/spss). Plots were conducted with GraphPad Prism (version 9, GraphPad Inc., San Diego, CA, USA).

Abbreviations

PD	Parkinson's Disease
DTI-ALPS	Diffusion tensor image analysis along the perivascular space
LPD	Left-onset PD
RPD	Right-onset PD
HCs	Healthy Controls
AI	Asymmetry index

Received: 29 September 2024; Accepted: 11 July 2025;
Published online: 24 July 2025

References

1. Bloem, B. R., Okun, M. S. & Klein, C. Parkinson's disease. *Lancet* **397**, 2284–2303 (2021).
2. Dickson, D. W. Neuropathology of Parkinson disease. *Parkinsonism Relat. Disord.* **46**, S30–s33 (2018).
3. Barrett, M. J., Wylie, S. A., Harrison, M. B. & Wooten, G. F. Handedness and motor symptom asymmetry in Parkinson's disease. *J. Neurol. Neurosurg. Psychiatry* **82**, 1122–1124 (2011).
4. Elkurd, M., Wang, J. & Dewey, R. B. Jr. Lateralization of motor signs affects symptom progression in Parkinson disease. *Front. Neurol.* **12**, 711045 (2021).

5. Wang, J. et al. MRI evaluation of asymmetry of nigrostriatal damage in the early stage of early-onset Parkinson's disease. *Parkinsonism Relat. Disord.* **21**, 590–596 (2015).
6. Bay, A. A., Hart, A. R., Michael Caudle, W., Corcos, D. M. & Hackney, M. E. The association between Parkinson's disease symptom side-of-onset and performance on the MDS-UPDRS scale part IV: Motor complications. *J. Neurol. Sci.* **396**, 262–265 (2019).
7. Verreyt, N., Nys, G. M., Santens, P. & Vingerhoets, G. Cognitive differences between patients with left-sided and right-sided Parkinson's disease. A review. *Neuropsychol. Rev.* **21**, 405–424 (2011).
8. Hanna-Pladdy, B., Pahwa, R. & Lyons, K. E. Paradoxical effect of dopamine medication on cognition in Parkinson's disease: relationship to side of motor onset. *J. Int Neuropsychol. Soc.* **21**, 259–270 (2015).
9. Ding, X. S. et al. Ferroptosis in Parkinson's disease: Molecular mechanisms and therapeutic potential. *Ageing Res. Rev.* **91**, 102077 (2023).
10. Brembati, V., Faustini, G., Longhena, F., Outeiro, T. F. & Bellucci, A. Changes in α-synuclein posttranslational modifications in an AAV-based mouse model of Parkinson's disease. *Int. J. Mol. Sci.* **24**, 13435 (2023).
11. Li, Y. et al. Plasma exosomes impair microglial degradation of α-synuclein through V-ATPase subunit V1G1. *CNS Neurosci. Ther.* **30**, e14738 (2024).
12. Djaldetti, R., Ziv, I. & Melamed, E. The mystery of motor asymmetry in Parkinson's disease. *Lancet Neurol.* **5**, 796–802 (2006).
13. Kempster, P. A., Gibb, W. R., Stern, G. M. & Lees, A. J. Asymmetry of substantia nigra neuronal loss in Parkinson's disease and its relevance to the mechanism of levodopa related motor fluctuations. *J. Neurol. Neurosurg. Psychiatry* **52**, 72–76 (1989).
14. Tysnes, O. B. & Storstein, A. Epidemiology of Parkinson's disease. *J. Neural Transm. (Vienna)* **124**, 901–905 (2017).
15. Riederer, P. et al. Lateralisation in Parkinson disease. *Cell Tissue Res.* **373**, 297–312 (2018).
16. Claassen, D. O. et al. Cortical asymmetry in Parkinson's disease: early susceptibility of the left hemisphere. *Brain Behav.* **6**, e00573 (2016).
17. Kim, J. S. et al. Topographic pattern of cortical thinning with consideration of motor laterality in Parkinson disease. *Parkinsonism Relat. Disord.* **20**, 1186–1190 (2014).
18. Pelizzari, L. et al. White matter alterations in early Parkinson's disease: role of motor symptom lateralization. *Neurol. Sci.* **41**, 357–364 (2020).
19. Zhu, Y. et al. Study of the relationship between onset lateralization and hemispheric white matter asymmetry in Parkinson's disease. *J. Neurol.* **270**, 5004–5016 (2023).
20. Xiao, Y., Peters, T. M. & Khan, A. R. Characterizing white matter alterations subject to clinical laterality in drug-naïve de novo Parkinson's disease. *Hum. Brain Mapp.* **42**, 4465–4477 (2021).
21. Zhang, X. et al. Topological patterns of motor networks in Parkinson's disease with different sides of onset: A resting-state-informed structural connectome study. *Front Aging Neurosci.* **14**, 1041744 (2022).
22. Iliff, J. J. et al. A paravascular pathway facilitates CSF flow through the brain parenchyma and the clearance of interstitial solutes, including amyloid β. *Sci. Transl. Med.* **4**, 147ra111 (2012).
23. Benveniste, H. et al. The Glymphatic System and Waste Clearance with Brain Aging: A Review. *Gerontology* **65**, 106–119 (2019).
24. Taoka, T. et al. Evaluation of glymphatic system activity with the diffusion MR technique: diffusion tensor image analysis along the perivascular space (DTI-ALPS) in Alzheimer's disease cases. *Jpn J. Radiol.* **35**, 172–178 (2017).
25. Bae, Y. J. et al. Altered brain glymphatic flow at diffusion-tensor MRI in rapid eye movement sleep behavior disorder. *Radiology* **307**, e221848 (2023).
26. Lee, H. J., Lee, D. A., Shin, K. J. & Park, K. M. Glymphatic system dysfunction in obstructive sleep apnea evidenced by DTI-ALPS. *Sleep Med.* **89**, 176–181 (2022).
27. Andica, C. et al. Neuroimaging findings related to glymphatic system alterations in older adults with metabolic syndrome. *Neurobiol. Dis.* **177**, 105990 (2023).
28. Zhang, Y. et al. Interaction between the glymphatic system and α-synuclein in Parkinson's disease. *Mol. Neurobiol.* **60**, 2209–2222 (2023).
29. Zou, W. et al. Blocking meningeal lymphatic drainage aggravates Parkinson's disease-like pathology in mice overexpressing mutated α-synuclein. *Transl. Neurodegener.* **8**, 7 (2019).
30. Cai, X. et al. Diffusion along perivascular spaces provides evidence interlinking compromised glymphatic function with aging in Parkinson's disease. *CNS Neurosci. Ther.* **29**, 111–121 (2023).
31. Si, X. et al. Neuroimaging evidence of glymphatic system dysfunction in possible REM sleep behavior disorder and Parkinson's disease. *NPJ Parkinsons Dis.* **8**, 54 (2022).
32. Li, Y. et al. The impact of sleep disorders on glymphatic function in Parkinson's disease using diffusion tensor MRI. *Acad. Radiol.* **32**, 2209–2219 (2025).
33. Ma, X. et al. Diffusion tensor imaging along the perivascular space index in different stages of Parkinson's disease. *Front. Aging Neurosci.* **13**, 773951 (2021).
34. Shen, T. et al. Diffusion along perivascular spaces as marker for impairment of glymphatic system in Parkinson's disease. *NPJ Parkinsons Dis.* **8**, 174 (2022).
35. Zhang, W. et al. Glymphatic clearance function in patients with cerebral small vessel disease. *Neuroimage* **238**, 118257 (2021).
36. Gu, L. et al. Noninvasive neuroimaging provides evidence for deterioration of the glymphatic system in Parkinson's disease relative to essential tremor. *Parkinsonism Relat. Disord.* **107**, 105254 (2023).
37. Sundaram, S. et al. Establishing a framework for neuropathological correlates and glymphatic system functioning in Parkinson's disease. *Neurosci. Biobehav. Rev.* **103**, 305–315 (2019).
38. Shin, N. Y. et al. Adverse effects of hypertension, supine hypertension, and perivascular space on cognition and motor function in PD. *NPJ Parkinsons Dis.* **7**, 69 (2021).
39. Lv, W. et al. Normal-sized basal ganglia perivascular space related to motor phenotype in Parkinson freezers. *Aging (Albany NY)* **13**, 18912–18923 (2021).
40. Morita, T., Asada, M. & Naito, E. Right-hemispheric dominance in self-body recognition is altered in left-handed individuals. *Neuroscience* **425**, 68–89 (2020).
41. Merrick, C. M. Left hemisphere dominance for bilateral kinematic encoding in the hum an brain. *Elife* **11**, e69977 (2022).
42. Zhu, M. & Cai, Q. Hemispheric co-lateralization of language and spatial attention reduces performance in dual-task. *Brain Lang.* **262**, 105537 (2025).
43. Li, K. et al. Abnormal spontaneous brain activity in left-onset Parkinson disease: a resting-state functional MRI study. *Front. Neurol.* **11**, 727 (2020).
44. Ren, J. et al. Glymphatic system dysfunction as a biomarker of disease progression in Parkinson's disease: neuroimaging evidence from longitudinal cohort studies. *J. Neurol.* **272**, 196 (2025).
45. Baumann, C. R., Held, U., Valko, P. O., Wienecke, M. & Waldvogel, D. Body side and predominant motor features at the onset of Parkinson's disease are linked to motor and nonmotor progression. *Mov. Disord.* **29**, 207–213 (2014).
46. Zhao, X. et al. The asymmetry of glymphatic system dysfunction in patients with temporal lobe epilepsy: A DTI-ALPS study. *J. Neuroradiol.* **50**, 562–567 (2023).
47. Iliff, J. J. et al. Cerebral arterial pulsation drives paravascular CSF-interstitial fluid exchange in the murine brain. *J. Neurosci.* **33**, 18190–18199 (2013).
48. Jiang-Xie, L. F. et al. Neuronal dynamics direct cerebrospinal fluid perfusion and brain clearance. *Nature* **627**, 157–164 (2024).

49. Nieuwenhuis-Mark, R. E. The death knoll for the MMSE: has it outlived its purpose?. *J. Geriatr. Psychiatry Neurol.* **23**, 151–157 (2010).
50. Andescavage, N. et al. In vivo assessment of placental and brain volumes in growth-restricted fetuses with and without fetal Doppler changes using quantitative 3D MRI. *J. Perinatol.* **37**, 1278–1284 (2017).
51. Amick, M. M., Grace, J. & Chou, K. L. Body side of motor symptom onset in Parkinson's disease is associated with memory performance. *J. Int. Neuropsychol. Soc.* **12**, 736–740 (2006).
52. Tomlinson, C. L. et al. Systematic review of levodopa dose equivalency reporting in Parkinson's disease. *Mov. Disord.* **25**, 2649–2653 (2010).

Acknowledgements

This work was supported by Nanjing Medical University-Qilu Clinical Research Fund Project [No. 2024KF0254], the National Natural Science Foundation of China [No. 82271273]. We are grateful to all of the study participants for their patience and cooperation.

Author contributions

Z.L.: conception and design of study, data acquisition, statistical analysis, writing original draft. X.M.: analysis and interpretation, data acquisition, statistical analysis. Q.Z.: conception and design of study, analysis and interpretation, revision of the paper. J.S.: data acquisitions, analysis, and interpretation, revision of the paper. Y.J.: conception and design of study, data acquisition. S.G.: data acquisitions, revision of the paper. P.J.: data acquisitions, revision of the paper. J.W.: data acquisitions, revision of the paper. K.Z.: conception and design of study, diagnosis and clinical evaluation, and obtaining funding. M.W.: conception and design of the study, revision of the paper, study supervision, and obtaining funding. All authors read and approved the final paper.

Competing interests

The authors declare no competing interests.

Additional information

Correspondence and requests for materials should be addressed to Min Wang.